

# Global Solution of the Finite Element Shape-from-Shading Model with a Bioluminescent Molecular Imaging Application

Jianghong Zhong, Jie Tian\*, *Fellow, IEEE*, Xin Yang, Chenghu Qin, *Member, IEEE*

**Abstract**—Only a planar bioluminescence image acquired from an ordinary cooled charge-coupled device (CCD) array every time, how to re-establish the three-dimensional small animal shape and light intensity distribution on the surface has become urgent to be solved as a bottleneck of bioluminescence tomography (BLT) reconstruction. In this paper, a finite element algorithm to solve the Dirichlet type problem for the first order Hamilton-Jacobi equation related to the shape-from-shading model is adopted. The algorithm outputting the globally maximal solution of the above problem avoids cumbersome boundary conditions on the interfaces between light and shadows and the use of additional information on the surface. The results of the optimization method are satisfied. It demonstrates the feasibility and potential of the finite element shape-from-shading (FE-SFS) model for reconstructing the small animal surface that lays one of key foundations for a fast low-cost application of the BLT in the next future.

## I. INTRODUCTION

Molecular imaging that unites molecular biology and *in vivo* imaging has emerged as a cornerstone discipline in the biomedical community [1], [2]. Optical molecular imaging has full use of molecular probes *in vivo*. The emitted light carries a wealth of biological information from the small animal surfaces. Bioluminescence tomography (BLT) that can acquire three-dimensional (3D) information of the *in vivo* light sources inside small animals has become a flagship product for optical molecular imaging [3], [4], [5], [6]. Although Wang, Klose and colleagues presented the uniqueness theorems in BLT about the light information from the surface to the inside *in vivo* [7], [8], how to obtain the surface light intensity distribution in mice by the detected planar bioluminescence image has not specially reported. At present, BLT mostly has to rely on computed tomography (CT) or Micro-CT, and laser scanner and so on to acquire 3D living surface data [9], [10], [11], [12]. Shortcomings are followed by the position changes of a live mouse and its different organs, the extension of imaging time, the increased cost of imaging equipments, and the imbalanced matching between the optical signal strength and the body surface. The finite element shape-from-shading (FE-SFS) model is such

an algorithm being developed in order to overcome the above problems by the optical molecular imaging system itself.

Lots of papers on the SFS problem have appeared since the classical publication by Horn and Brooks, which seem to be the most representative in three classes: methods of resolution of partial differential equations, methods using minimization and methods approximating the image irradiance equation[13]. It is the fact that the SFS problem deserves analysis despite the simplicity of its formulation and satisfactory approaches is still lacking with a global method for its resolution under realistic assumptions. Many technical questions such as the uniqueness of solutions without continuity assumptions remain open. Mathematical tools and numerical techniques that involve non-smooth solutions and boundary conditions, and guarantee convergence to an approximate solution under rather broad assumptions, are developed quickly these years. The FE-SFS model is an outcome of these advances, which integrates the finite element, an unique continuous viscosity solution of the eikonal equation, and the maximal solution with shadows into a method that will be detailed in the following.

The organization of the paper is as follows. The next section introduces the proposed FE-SFS algorithm. The experiments and results of the 3D surface reconstruction are thoroughly demonstrated in Section 3. Section 4 concludes the paper and discusses future works.

## II. ALGORITHMS

The FE-SFS model about the two-dimensional (2D) images can be derived by the image radiation equation [13], [14]

$$\Gamma(\vec{n}(x, y)) = I(x, y), \quad (1)$$

where  $I(x, y)$  is the light intensity measured at the point  $(x, y)$  in the domain of the Lambertian surface  $s$  given as a graph  $g = s(x, y)$  with  $x, y \in R$ ,  $\vec{n}(x, y)$  is the unit normal to the surface at the corresponding point and  $\Gamma(\vec{n}(x, y))$  is the reflection map giving the value of the light reflection on the surface as a function of its normal orientation at each point.  $I(x, y)$  takes double values in the interval  $[0, 1]$  so as to construct a continuous model. Let's assume that there is a unique light source at infinity, of which the direction is indicated by the unit vector  $\omega = (\omega_1, \omega_2, \omega_3) \in R^3$ , and  $s$  has a compact support  $\Omega$ . Then, we can describe the reflection map as  $\Gamma(\vec{n}(x, y)) = \vec{n}(x, y) \cdot \omega$ . Equation (1) can be rewritten in the form

$$I(x, y)\sqrt{1 + |\nabla s(x, y)|^2} + l(x, y) = 0, \quad (2)$$

$$l(x, y) = (\omega_1, \omega_2) \cdot \nabla s(x, y) - \omega_3, (x, y) \in \Omega. \quad (3)$$

This paper is supported by the Project for the National Basic Research Program of China (973) under Grant No.2006CB705700, the Knowledge Innovation Project of the Chinese Academy of Sciences under Grant No. KGCX2-YW-907, Changjiang Scholars and Innovative Research Team in University (PCSIRT) under Grant No.IRT0645, CAS Hundred Talents Program, Science and Technology Key Project of Beijing Municipal Education Commission under Grant No. KZ200910005005.

Medical Image Processing Group, Institute of Automation, Chinese Academy of Sciences, Beijing, 100190, China

\* Corresponding author: Jie Tian; Telephone: 8610-82628760; Fax: 8610-62527995. tian@ieee.org

(2) is a first order nonlinear partial differential equation of Hamilton-Jacobi type. Meanwhile, we complement (2) with the natural Dirichlet boundary condition

$$s(x, y) = 0, (x, y) \in \partial\Omega, \quad (4)$$

which means that the surface is standing on a background. The solution of above Dirichlet problem shall give a surface corresponding to the brightness  $I(x, y)$  measured in the image representing  $\Omega$ .

Let us consider the case of a vertical light,  $\omega = (0, 0, 1)$ . The general equation (2) turns into

$$I(x, y)\sqrt{1 + |\nabla s(x, y)|^2} - 1 = 0. \quad (5)$$

We write (4), (5) in explicit out an array

$$\begin{cases} |\nabla s(x, y)| = f(x, y), & (x, y) \in \Omega \\ s(x, y) = 0, & (x, y) \in \partial\Omega \end{cases} \quad (6)$$

$$f(x, y) = \sqrt{-1 + 1/I(x, y)^2}, 0 < I(x, y) < 1. \quad (7)$$

Note that there is no shadow with a vertical light since our surface is a graph and  $I(x, y)$  can only vanish at points of maximum brightness where  $f(x, y) = 0$ . This causes the lack of uniqueness of classical viscosity solutions. So a new variable  $\nu(x, y) = 1 - e^{-s(x, y)}$  is introduced to obtain an approximation scheme in the form of a fixed point problem, according to the results by Ishii-Ramaswamy and M.Sagona. The problem for  $\nu(x, y)$  becomes

$$\begin{cases} \nu(x, y) + \max\{\varphi(x, y)\} = 0, & (x, y) \in \Omega \\ \varphi(x, y) = -\frac{a}{f(x, y)} \cdot \nabla \nu(x, y) - 1 & (x, y) \in \Omega \\ a \in B_2(0, 1) \\ \nu(x, y) = 0, & (x, y) \in \partial\Omega. \end{cases} \quad (8)$$

It is proved that (8) has a unique continuous viscosity solution provided  $f$  is bounded and never vanishes in  $\Omega$ .

In the FE-SFS model with a mesh of the set  $\Omega_\delta = \Omega + \delta B_2(0, 1)$ , we assume that the image is a rectangle  $\Omega \subset R^2$ .  $\Upsilon_{in}$  is the set of indices of the nodes  $p_i = (x_i, y_i) \in \Omega$ , while  $\Upsilon_{out}$  is the set of indices of the nodes  $p_i \in \Omega_\delta \setminus \Omega$ . Then, their union is  $\Upsilon$  and  $N$  is the number of total nodes. Let  $k$  be the size of the mesh and  $E^k$  denote the space of linearly piecewise affine functions on the cells. It is our aim that is to find a solution  $\epsilon \in E^k$  of

$$\begin{cases} \epsilon(p_i) = \min\{e^{-h}\epsilon v(p_i)\} + 1 - e^{-h}, & i \in \Upsilon_{in} \\ v(p_i) = p_i + h\frac{a}{f(p_i)}, & i \in \Upsilon_{in} \\ \epsilon(p_i) = 0, & i \in \Upsilon_{out}. \end{cases} \quad (9)$$

M. Falcone proved that the FE solution of (9) existed and it was unique. The FE solution of our problem can be acquired by a fixed point iteration on the operation  $\Phi : R^N \rightarrow R^N$

$$(\Phi)_i \equiv \begin{cases} \min\{e^{-h}P(a)A\}_i + 1 - e^{-h}, & i \in \Upsilon_{in} \\ 0, & i \in \Upsilon_{out} \end{cases} \quad (10)$$

where  $A$  is the  $N$  dimensional vector containing the values at the nodes of the mesh, and  $P(a)$  is the matrix of the local coordinates of the points  $v(p_i)$ . In summary, the FE-SFS model will converge monotonically to the globally maximal solution.

The final part will explain why we can use the same equation everywhere in  $\Omega$  without introducing any boundary condition in the *light* region  $\Omega_{light}$ . Although the boundary of the *light* region may be non-smooth or not belong to the mesh while the light is oblique,  $I(x, y) = 0$  in the *shadow* region  $\Omega_{shadow}$ . Here,  $\Omega = \Omega_{light} \cup \Omega_{shadow}$ . In an other word, we only need to solve the equation

$$l(x, y) = 0, (x, y) \in \Omega_{shadow}. \quad (11)$$

Equation (11) clearly coincides with (2). So we will have a similar operator with the same properties of  $T$  corresponding to the oblique light, while the numerical approximation of the maximal solution with shadows is also satisfied using the FE-SFS model.

### III. EXPERIMENTS AND RESULTS

In order to display a complete process, the section will demonstrate a *in vivo* mouse experiment and its results. The work was all implemented on a computer with Intel Core(TM)2 Duo Processor 2.33GHz and 2GB RAM.

*Fig.1* included a bioluminescent image (*Fig.1(a)*) and the corresponding photographic image (*Fig.1(b)*) derived from the same perspective. The pair of images was processed using a robust image modeling technique [15] to be restored and segmented. In the experiment, the Nu/Nu nude mouse subcutaneously transplanted tumor cells was anesthetized by 2% isoflurane delivered in medical air, and scanned in the optical molecular imaging system, WinMI. WinMI was calibrated with the help of USS-1200V-LL Integrating Spheres. Hence, we simultaneously obtained the corresponding light intensity at the surface area of small animals. In order to reconstruct the 3D surface of the small animal using the FE-SFS model, the binary image (*Fig.1(c)*) of the photograph was created.

A gray-scale transformation of the photographic image was processed to reconstruct the surface on the small animal using the FE-SFS model. The transformation function was defined as follows

$$\tilde{I}(x, y) = \begin{cases} I(x, y), & 0 \leq I(x, y) \leq I_0 \\ I_0, & I_0 \leq I(x, y) \leq 1. \end{cases} \quad (12)$$

Then,  $\tilde{I}(x, y)$  and the binary image were used as the inputs in the FE-SFS model.

*Fig.2* and *Fig.3* were the 3D surface as outputs of the FE-SFS model. The 3D digital mouse was discretized by tetrahedron elements with 17996 triangles, 180190 tetrahedrons, and 35439 nodes in *Fig.2* and *Fig.3*. In the experiment, the step for  $x, y, z$  axis was 0.015cm showing in *Fig.2* and *Fig.3*, while  $I_0 = 0.99$  during the computing phase. The number of the total iteration was 1887, while the total time cost by the proposed algorithm in the paper was 44 seconds with the mean absolute deviation error 1%. The maximum height of the reconstructed surface from the background was 2.94cm. Finally, the energy at every node of the finite element mesh in the direction of orthogonal projection was set by the bioluminescent image, because of assuming that there was only a uniquely vertical light source. The result was illustrated in *Fig.4*. *Fig.5* was the enlarged one of *Fig.4* so as to be clearly observed.

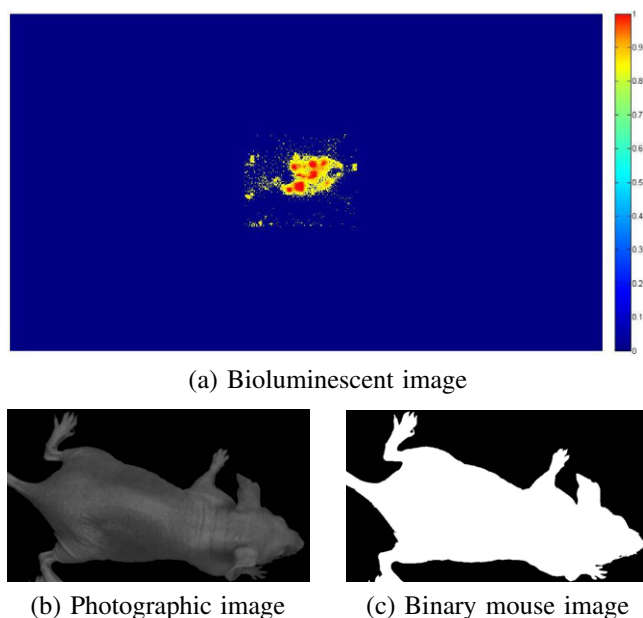


Fig. 1. The *in vivo* bioluminescent image with the corresponding photographic image was derived from the same perspective, as the input of the FE-SFS model. (a) is the bioluminescent image of the mouse; (b) is the photographic image; (c) is the binary image of the photograph.

#### IV. CONCLUSIONS AND FUTURE WORKS

##### A. Conclusions

The *in vivo* experiments were performed to verify the FE-SFS model and 3D surface light intensity distribution in mice can be reconstructed by 2D images from only one perspective. Given the difficulty that there is no unique solution to the eikonal equation of the SFS problem in general case, and the need for fast low-cost BLT reconstruction algorithm, we have developed and applied the FE-SFS algorithm. The global solution of the Dirichlet type problem in FE-SFS model was a unique viscosity solution, although it was only an approximate of the maximal solution of the eikonal equation. The application of FE-SFS model in BLT presented in the paper may be useful for the fast low-cost molecular imaging.

##### B. Future Works

Our method currently required a special border region of lighting area that limits potential applications. We default that the height of light areas adjacent to the shadow or background is zeros. In fact, it is not always true. For example, the mouse's ears should be erected, but what we get is attached to the ground in Fig.3 or Fig.4. Another disadvantage is that the surface of the mouse is not smooth,



Fig. 2. The reconstructed finite element mesh with 17996 triangles, 180190 tetrahedrons, and 35439 nodes by the FE-SFS method, using only one 2D photographic image. a, b, and c are the XY, YZ, and ZX plane of the tetrahedron elements respectively.

compared with the real mouse. As you known, the back of the mouse should be more relatively flat. Therefore, there are a lot of interesting work waiting for us to improve the FE-SFS model.

#### V. ACKNOWLEDGMENTS

The authors would like to thank Department of Laboratory Animal Science, Peking University Health Science Center for providing the Nu/Nu nude mice during experiments.

#### REFERENCES

- [1] R. Weissleder and M.J. Pittet, Imaging in the Era of Molecular Oncology, *Nature*, vol. 452, 2008, pp 580-589.
- [2] D. Hoeller and I. Dikic, Targeting the Ubiquitin System in Cancer Therapy, *Nature*, vol. 458, 2009, pp 438-444.
- [3] V. Ntziachristos, J. Ripoll, L. V. Wang, and R. Weissleder, Looking and listening to light: the evolution of whole body photonic imaging, *Nat. Biotechnol.*, vol. 23, 2005, pp 313-320.
- [4] J.K. Willmann, N.V. Bruggen, L.M. Dinkelborg and S.S. Gambhir, Molecular imaging in drug development, *Nature*, vol. 7, 2008, pp 591-607.
- [5] J. Tian, J. Bai, X.P. Yan, S.L. Bao, Y.H. Li, W. Liang, and X. Yang, Multimodality Molecular Imaging, *IEEE EMBM.*, vol. 27, 2008, pp 48-57.
- [6] G. Wang, W. Cong, H. Shen X. Qian, M. Henry and Y. Wang, Overview of bioluminescence tomography—a new molecular imaging modality, *Front Biosci.*, vol. 13, 2008, pp 1281-1293.
- [7] G. Wang, Y. Li, and M. Jiang, Uniqueness theorems in Bioluminescence Tomography, *Med. Phys.*, vol. 31, 2004, pp 2289-2299.
- [8] A.D. Klose, V. Ntziachristos, and A.H. Hielscher, The Inverse Source Problem based on the Radiative Transfer Equation in Optical Molecular Imaging, *J. Comput. Phys.*, vol. 202, 2005, pp 323-345.
- [9] J. Virostko, A. C. Powers, and E. D. Jansen, Validation of luminescent source reconstruction using single-view spectrally resolved bioluminescence images, *App. Opt.*, vol. 46, 2005, pp 2540-2547.
- [10] J.C. Feng, K.B. Jia, C.H. Qin, G.R. Yan, S.P. Zhu, J.T. Liu, and J. Tian, Three-dimensional Bioluminescence Tomography based on Bayesian Approach, *Opt. Express*, vol. 17, 2009, pp 16834-16848.

- [11] Y.J. Lu, X.Q. Zhang, A. Douraghy, D. Stout, J. Tian, T.F. Chan and A.F. Chatzioannou, Source reconstruction for spectrally-resolved bioluminescence tomography with sparse a priori information, *Opt. Express*, vol. 17, 2009, pp 8062-8080.
- [12] K. Liu, J. Tian, X. Yang, Y.J. Lu, C.H. Qin, S.P. Zhu, and X. Zhang, A Fast Bioluminescent Source Localization Method based on Generalized Graph Cuts with Mouse Model Validations, *Opt. Express*, vol. 18, 2010, pp 3732-3745.
- [13] J.D. Durou, M. Falcone and M. Sagona, Numerical methods for shape-from-shading: A new survey with benchmarks, *CVIU.*, vol. 109, 2008, pp 22-43.
- [14] A. Tankus, N. Sochen and Y. Yeshurun, A New Perspective [on] Shape-from-Shading, *Proceedings of the Ninth IEEE International Conference on Computer Vision (ICCV 2003)*, Nice, France 2003, vol.2.
- [15] J.H. Zhong, R.P. Wang and J. Tian, Robust image modeling technique with a bioluminescence image segmentation application, in *Proceedings of SPIE Symposium on Medical Imaging 2009*, Lake Buena Vista, Florida, USA 2009, pp. 7262.

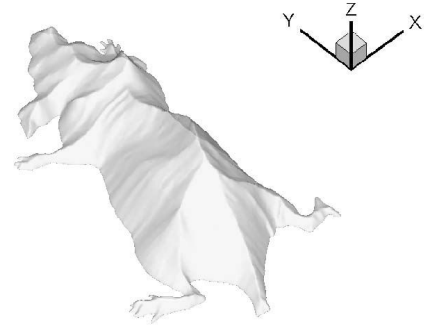


Fig. 3. The reconstructed surface by the FE-SFS method, using only one 2D photographic image. The mouse was discretized by tetrahedron elements with 17996 triangles, 180190 tetrahedrons, and 35439 nodes.

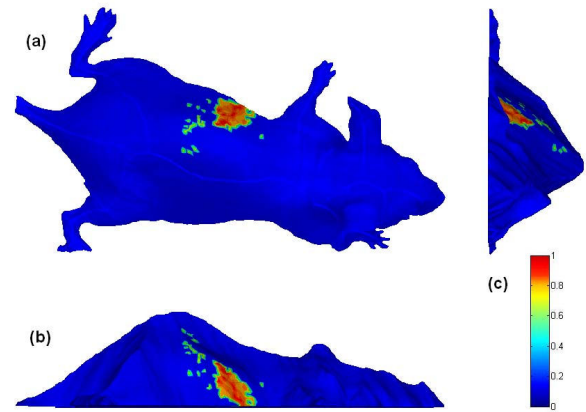


Fig. 4. The bioluminescence distribution on the mouse surface reconstructed by the FE-SFS method, using the 2D bioluminescent image and photographic image. a, b, and c are the XY, YZ, and ZX plane of the surface respectively.

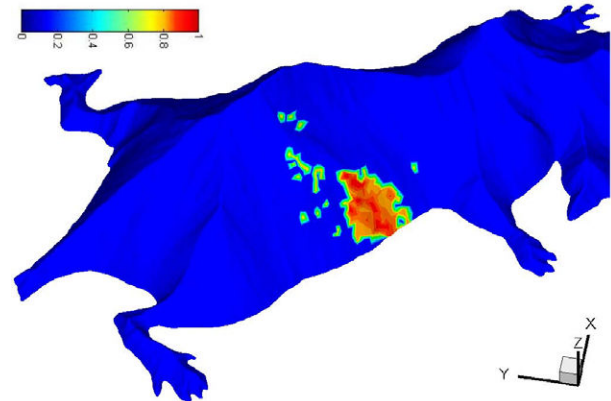


Fig. 5. The local image of the reconstructed mouse with the bioluminescent surface distribution by the FE-SFS method.